inorganics

MDPI

Perspective

Silicon Anode: A Perspective on Fast Charging Lithium-Ion Battery

Jun Lee [1,†], Gwangeon Oh [2,†], Ho-Young Jung [3,*] and Jang-Yeon Hwang [2,4,*]

[1] Department of Materials Science and Engineering, Chonnam National University, Gwangju 61186, Republic of Korea
[2] Department of Energy Engineering, Hanyang University, Seoul 06407, Republic of Korea
[3] Department of Environment and Energy Engineering, Chonnam National University, Gwangju 61186, Republic of Korea
[4] Center for Energy Storage System, Chonnam National University, Gwangju 61186, Republic of Korea
* Correspondence: jungho@chonnam.ac.kr (H.-Y.J.); jangyeonhw@hanyang.ac.kr (J.-Y.H.)
† These authors contributed equally to this work.

Abstract: Power sources supported by lithium-ion battery (LIB) technology has been considered to be the most suitable for public and military use. Battery quality is always a critical issue since electric engines and portable devices use power-consuming algorithms for security. For the practical use of LIBs in public applications, low heat generation, and fast charging are essential requirements, but those features are still unsatisfactory so far. In particular, the slow Li^+ intercalation kinetics, lithium plating, and self-heat generation of conventional graphite-anode LIBs under fast-charging conditions are impediments to the use of these batteries by the public demands. The use of silicon-based anodes, which are associated with fast reaction kinetics and rapid Li^+ diffusion, has great potential to render LIBs suitable for public use in the near future. In this perspective, the challenges in and future directions for developing silicon-based anode materials for realizing LIBs with fast-charging capability are highlighted.

Keywords: lithium-ion batteries; fast-charging; graphite anode; silicon anode

Citation: Lee, J.; Oh, G.; Jung, H.-Y.; Hwang, J.-Y. Silicon Anode: A Perspective on Fast Charging Lithium-Ion Battery. *Inorganics* **2023**, *11*, 182. https://doi.org/10.3390/inorganics11050182

Academic Editor: Moulay T. Sougrati

Received: 24 February 2023
Revised: 6 April 2023
Accepted: 17 April 2023
Published: 24 April 2023

1. Introduction

Lithium-ion batteries (LIBs) are an established technology for energy-storage and have the potential for small to large-scale applications because of their high energy density, high specific energy, and good recharge capability [1]. Notably, they are currently the best power sources in terms of portability for small consumer electronics such as laptops and smartphones. Battery-powered electric vehicles (EVs) are coming into the limelight and their market share is increasing rapidly [2–4]. The International Energy Agency has predicted that the global EV industry will grow rapidly over the next decade and that by 2030, the global EV stock will reach 230 million [5–7]. In 2021, the sales of EVs increased by 108% compared with the crisis year of 2020, and it has been predicted that the sales growth will touch 129% at the end of 2022 compared with 2021 based on previous reports [8–10] (see the Figure 1).

In addition to public demands, the electrification of military transportation is increasing. In the case of drone systems, a major objective is to develop high-power LIBs to extend the flying range by several hundred percent. Reconnaissance drones, which are among the latest technologies, are being deployed on a regular basis for ensuring safety and monitoring purposes following increased hostilities along some international borders. Importantly, the drones should be sufficiently light to be effective and efficient and to have a long flight time to complete mission objectives, since they cannot carry conventional batteries, which are heavy and offer only short flight capability [11].

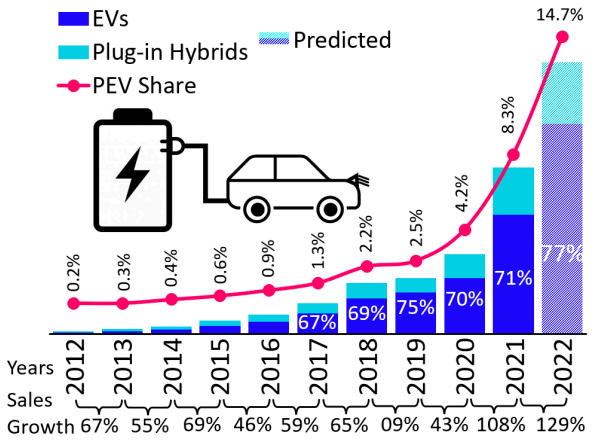

Figure 1. Global EV sales and development trends from 2012 to 2021 [Reprinted with permission from Ref. [8]. Copyright, 2022 John Wiley & Son, Inc] and prediction for 2022 from Ref. [10].

However, LIBs have many drawbacks such as a long recharging time, dendrite formation on the anode, mechanical crack formation, and self-heat generation. Therefore, the development of LIBs with fast-charging capability, heat control, and dendrite-free anode is important to promote the commercialization of EVs [9,12–14]. On the other hand, in military applications, it is imperative to address the aforementioned drawbacks since the overall battery characteristics, including its lifespan and fast-charging capability, are critical for supporting military missions (Figure 2a). Despite the significant advances in the use of LIBs for small and medium-sized devices and even EVs, therefore, current LIBs are not widely used for military purposes because of their slow charging and safety issues [15]. While high-power batteries that can discharge at even 15 C have been reported [16], the charging rate of most LIBs containing a carbon-based anode is close to 3 C. In fact, the poor kinetics and low operating potential (0.1 V vs. Li/Li^+) of graphite-base anodes lead to serious issues during fast charging, such as mechanical cracks [17,18], electrolyte decomposition [19,20], anode polarization that induces dendrite formation [21,22], and self-heat generation [2,23], which drastically degrade the battery performance and give rise to safety issues.

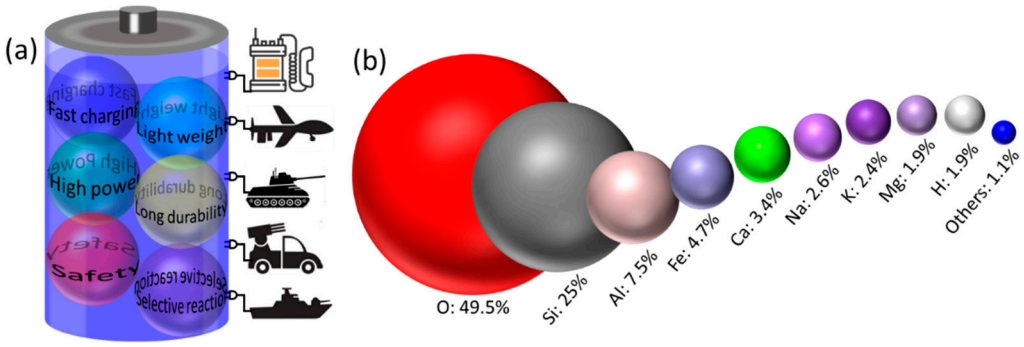

Figure 2. (**a**) Key properties of LIBs that required to make them suitable for military applications and (**b**) abundance of elements in the earth's crust (ball area reflectings the relative amount).

To overcome these drawbacks, new materials have been introduced for developing fast-charging anodes; particularly, nano-scaled silicon has been emerging as a potential candidate [24–26]. Silicon-based anodes have an energy capacity that is about 11 times higher than that graphite-based anodes. Moreover, silicon element is not only abundant in the earth's crust (it is the second most abundant element) (Figure 2b) but also relatively inexpensive and safe. Furthermore, it has a low discharge potential (≈0.37 V vs. Li/Li^+) [25]. However, most of the silicon-based anodes have the drawbacks of huge volume expansion (≈400%) [27], poor electronic conductivity ($\approx 10^{-3}$ S cm^{-1}) [28], and a low Li^+ diffusion rate ($\approx 10^{-13}$ cm^2 s^{-1}) [29], and it is necessary to overcome these drawbacks if the anodes

are to be used in military applications. Numerous strategies have been proposed for buffering the volume expansion (Figure 3a) [30], including thin-film preparation, pore formation, and the use of shape-preserving shell designs that can accommodate volumetric changes. For conductivity enhancement, the addition of carbon materials is a common method (Figure 3b) [31] since carbon nanomaterials have excellent electrical and ionic conductivity apart from useful mechanical properties [32,33] as well various structural designs in anode materials for LIBs [34–36]. Additionally, morphological tuning through the use of nanoparticles, nanowires, nanospheres, and/or nanotubes is considered the promising strategy for Si-based anodes for LIBs. Here, we discussed research progress on and the development of fast-charging silicon-based anode materials for rechargeable LIBs.

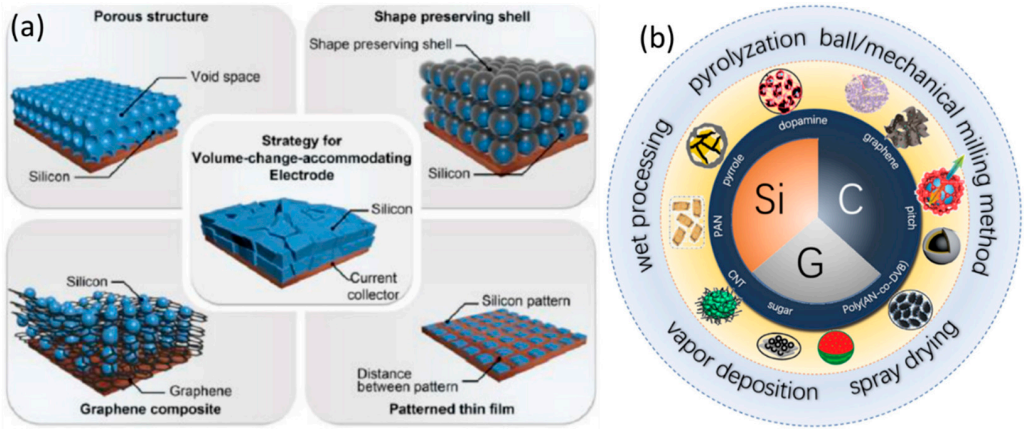

Figure 3. (**a**) Recommended strategies for buffering the large volume change in silicon anodes during cycling (Reprinted with permission from Ref. [30]. Copyright, 2015 John Wiley & Sons, Inc, Hoboken, NJ, USA) and (**b**) suggested approach and representative structures of silicon/carbon composite anodes prepared with various methods for increasing conductivity (Reprinted with permission from Ref. [31]. Copyright, 2019 John Wiley & Sons, Inc).

2. Key Considerations to Achieve Fast Charging

In order to design materials that can quickly charge LIB anodes, we need first to investigate the operating principle of LIBs and carefully identify the stages that are restricting the charging rate in order to optimize the kinetics of the electrochemical process. First, Li^+ ions diffuse into the bulk of the layered oxide cathode via the cathode/electrolyte interface (CEI); second, Li^+ is solvated by the solvent molecules at the CEI-electrolyte interface; and third, the solvated Li^+ ions diffuse into the bulk electrolyte via mesopores and tortuous channels in the cathode and anode; Fourth, Li^+ ions in a solvate are desolvated at the anode/electrolyte interface (commonly referred to as the solid electrolyte interphase, SEI); fifth, Li^+ ions pass through the SEI and penetrate the graphite lattice; sixth and final, Li^+ ions diffuse within the bulk of graphite, and the diffusion is accompanied by the rearrangement of the graphite lattice (Figure 4a). The kinetics of the Li^+ ions during this process must be quick enough to maintain a high rate of charge. Materials that can charge quickly and efficiently should have low energetic barriers for Li^+ migration into them and low energy barriers for Li^+ diffusion inside the bulk of the materials (Figure 4b).

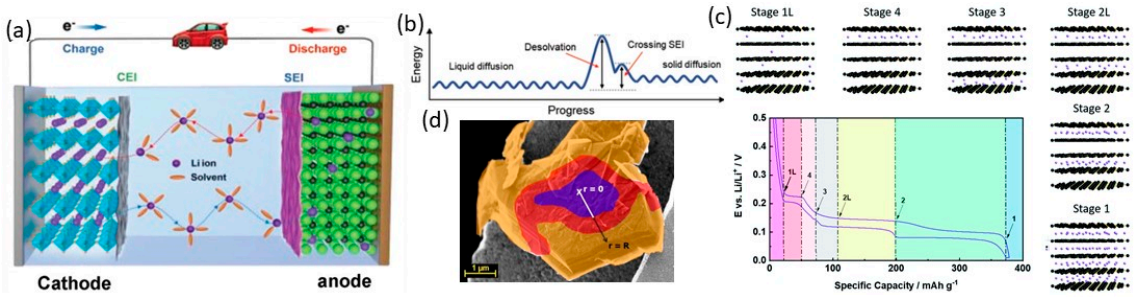

Figure 4. (**a**) Working principle of LIBs, (**b**) the energy diagram of their charging process (Reprinted with permission from Ref. [8]. Copyright, 2022 John Wiley & Sons, Inc), (**c**) illustration of the electrochemical lithiation/delithiation mechanism of Li^+ ions into the graphite lattice (inset: the given representative potential profile refers to the second discharge/charge cycle in the half-cell configuration (Reprinted with permission from Ref. [26]. Copyright, 2020 Royal Society of Chemistry, London, UK), (**d**) a schematic illustration of the "shrinking annuli model" for a single crystal graphite particle (Reprinted with permission from Ref. [37]. Copyright, 2013 Elsevier, Amsterdam, The Netherlands).

2.1. Conductivity of Materials

For the LIB anode performance to be high, the anode material should have high Li^+ storage capacity apart from rapid ionic conductivity and high electronic conductivity. Furthermore, large volumetric changes should not occur during cycling. A number of materials, including carbon, metals, and alloys, show promise as fast-charging anode materials due to their high intrinsic electrical conductivity and small or zero band gaps. External manipulations including heating, conductive doping, coating with conductors, altering the size and shape, and doping with heteroatoms are also crucial. It is known that coating conductive anode materials with conductive agents enhances electron diffusion. Furthermore, tuning the band gap through the incorporation of heteroatoms through functionalization or doping can significantly enhance the electronic conductivity of the anode material [38].

According to energy band theory, for an anode material to act as a conductor, electrons in the valence band of the material should cross the forbidden band and enter the conduction band. The electron conduction property is generally characterized by the electron mobility σ, which is regarded as an important parameter. Since solid anode materials include both holes and free electrons, we can express σ as

$$\sigma = n_i e \mu_e + P_i e \mu_h \quad (1)$$

where n_i and P_i are the concentrations of electrons and holes, respectively, μ_e is the mobility of electrons, and μ_h is the mobility of holes.

2.2. Ion Diffusivity of Materials

The fast diffusion rate of Li^+ is another critical aspect that affects the fast-charging capability of anode materials. The below mentioned Ar-rhenius equation will be used to describe the diffusion process of Li^+, and the diffusion coefficient (Di), represents the diffusion flow per unit.

$$D_i = D_0 \exp(-\Delta G/(K_B\, T)) \quad (2)$$

where D_0 is the maximum value of diffusivity, ΔG is the activation energy of diffusion, K_B is the Boltzmann constant, and T is the temperature.

Therefore, to boost the Li^+ diffusion kinetics and electron transport, identifying suitable anode materials with high D_i, preparing thin electrodes for reducing material loading, and tuning structural features can help develop fast-charging anodes for LIBs (Figure 4).

2.3. Stable SEI Formation

In spite of the merits as a next generation anode due to its high reversible capacity, the large volumetric changes that occur during lithiation and delithiation provide specific hurdles for the formation of stable SEI layers on silicon anodes. The huge volumetric differences not only contribute to severe mechanical challenges, but also lead to poor stability of the SEI. Therefore, the SEI that works best for silicon anodes is not the same as the one that works best for graphite anodes. For SEI on silicon anodes, both good ionic conductivity and great elasticity are requirements [39]. FEC, which creates an SEI with both high concentrations of LiF and an elastic polymer, is one of the electrolyte additives that is utilized for silicon anodes the most frequently. By gaining a deeper understanding of the stability that is provided by this polymer-inorganic composite surface film, we will be able to create superior interfacial polymer-inorganic composite surface films, which will, in turn, improve the cycling performance of silicon anodes. These interface films may have originated either from prefabricated interfaces or from the breakdown reactions of additives to the electrolyte. The formation of a prepared SEI by the interaction of binders with the surface of silicon anodes can result in an improvement in the performance of silicon anodes. Consequently, the research and development of superior binders for silicon anodes is another viable option [40].

2.4. Electrolyte Modification

Electrochemical reactions mainly take place in electrode/electrolyte interface, SEI layer property decides overall LIBs characteristics; power capability, and cyclability. The nature of electrolytes determines interface properties, suitable choice of salt, solvent, and additive are major issues. For example, Zeng et al. [41] introduced solvent modification. Unlike simple carbonates and ether solvents, fluorinate carbon-based concentrate electrolytes significantly improved safety, and initial columbic efficiency. 4.3 M LIFSI/FEC-TFEC deliver 0.064% capacity fading rate per cycle and 1312 mAh g^{-1} at 8 A g^{-1}. Additive research is conducted by Han et al. [42]. By adding 0.1 M $M(TFSI)_x$ (M = Mg, Zn, Al, Ca) as a second salt into the electrolyte, make an in situ formation of Li-M-Si ternary phased during cycling.

3. Graphite Anode

Graphite is a form of intercalation material that could also accept or release Li+ ions from the bulk electrode. Typically, carbon materials exist in either sp^3 or sp^2 electronic hybridization. In the case of sp^2 hybridization of graphene, sp^2 hybridized sheets are linked by π–π interactions rather than weak van der Waals forces. It is usually by π–π interactions that connect hybridized graphene, and the weak van der Waals force between graphene layers allows ions to be intercalated [26]. Bulk-layered graphite can be formed by stacking these layers in either an ABAB sequence with hexagonal symmetry or an ABCABC sequence with rhombohedral symmetry. It is the layered structure of graphite that allows for the existence of basal planes and edge planes on graphite particles. Generally, the prismatic plane has higher surface energy than the basal plane, which leads to higher surface reactivity. However, the weak van der Waals forces between the graphene layers facilitate the intercalation of ions. As early as 1840, the notion of such graphite intercalation compounds (GICs) had been established.

Graphite's application as an active material in the negative electrode of LIBs for the reversible intercalation of Li+ has received a lot of commercial interest since 1983 [43]. Stage 1 (Figure 4c) is the terminal stage of Li^+ intercalation and follows the basic mechanism of deintercalation/intercalation. Both the theoretical specific capacity of 372 mA h g^{-1} and the volumetric capacity of 850 mA h cm^{-3} are accounted for at this point. It has been shown that at high Li concentrations, graphene layers slightly slide with regard to one another, resulting in a switch in orientation from the original ABABA sequence of pristine graphite to the more complex AIAIA sequence of completely lithiated graphite (LiC_6) [44].

Specifically, Heß and Novak [37] looked at the kinetic performance of Li^+ diffusion through crystalline graphite particles (1 mm thick electrode). In contrast to the intensively lithiated phases, the liquid-like stages had a significantly different Li^+ diffusion coefficient. For instance, during lithiation at high current rates, full capacity may not be attained while passing from Stage 2L to Stage 2. Over potential rises as a result of diffusion limits, and Stage 1 nucleates at the edge planes of the graphite particle. To further understand this behavior, we have color-coded an arbitrary graphite particle (shown in Figure 4d) at three distinct stages: gold for stage 1, red for stage 2, and blue for stage 2L.

4. Titanium-Based Materials: Lithium Titanate (LTO)

$Li_4Ti_5O_{12}$ (LTO) anode is a promising material for lithium-ion battery systems. LTO structure is spinel material and undergoes two-phase reaction (LTO-$Li_7Ti_5O_{12}$(LI_7)) during charge and discharge process. LTO undergoes zero volume change and has a relatively stable charge storage voltage (~1.55 V vs. Li^+/Li) during cycling [45,46]. Therefore, The LTO anode material can exhibit high structural stability and power performanceduring. A simple sol-gel technique was used to manufacture core-shell-structured Si-based multi-components, with the Si surface evenly covered with double-shell coating layers of lithium silicate (Li_2SiO_3 and $Li_2Si_2O_5$, designated LS) and lithium titanate ($Li_4Ti_5O_{12}$, abbreviated LTO). The increased surface area of the Si-multicomponent is due in part to the void areas between the crystalline Layers. Because of this, the surface area of Si-multi-50 is larger than that of pure Si. When LTO capacities grew, the surface area of Si-multi-components expanded to accommodate them. Atom-selective in situ Ti K-edge XAFS characterization can be performed during the first lithiation to directly identify the function of the surface LTO layer in the improved kinetic electrochemical performance of the surface-modified Si anode material. In addition, the LTO-coated Si anode material's rate capability can be improved by rapid Li-ion conduction at the interface area, as a result of the lithiated $Li_7Ti_5O_{12}$ surface layer's increased electrical conductivity due to the mixed valence state of Ti^{3+}/Ti^{4+} [47].

Xia et al. [48] introduced Si@LTO@C provides a reversible capacity of 848 mA h g^{-1} with a current density of 15 A g^{-1} after 1000 cycles at 80 °C and is used as the anode material in Li-ion batteries (Figure 5). Micro-sized Si@LTO@C is therefore claimed to be a promising electrode material for high-performance LIBs, particularly in a harsh environment.

Figure 5. Schematic illustration showing the synthetic process of the Si-based multi-components. (Reprinted with permission from Ref. [47]. Copyright, 2015 Royal Society of Chemistry).

5. Silicon Anode

Silicon is one of the best alternatives to carbon because of its abundance in nature, low cost, and toxic-free and environmentally friendly nature. Multiple alloying reactions with Li per single atom (Li-Si formation) produce a high specific capacity, which can lead to a reduction in the thickness of the electrode without impacting the overall energy density [49,50]. Moreover, importantly, this unique feature can enhance the fast-charging process by reducing the concentration and potential gradient effects. Concentration and potential gradient effects can impair fast-charging in the intercalation-based graphite anode due to an electric potential gradient between the surface layer and the bulk. The concentration and potential gradient effects are worse in highly charged states when the

anode is completely lithiated [51]. Instead of intercalation between layers, lithium ions are alloying elements into the silicon lattice in the silicon anode. This means that lithium-ion buildup does not occur in highly charged states, when the anode is completely lithiated, which reduces electric potential gradient resistance during fast charging. Silicon anodes have a substantially greater Li storage potential than graphite (0.22 V vs. Li^+/Li for silicon vs. 0.1 V for graphite), which reduces the possibility of lithium concentration gradient effects during fast charging. This can minimize capacity degradation while cycling [52].

Li ions begin penetrating Si particles (around 0.1 V) to complete the alloy reaction; the penetration continues until the voltage drops to 0.01 V, and the result is per Si-atom consisting of 4.4 Li^+ during the lithiation process. This process begins with the formation of a solid-electrolyte interface (SEI) film on the Si surface above 0.5 V. However, the poor intrinsic conductivity of silicon (1.56×10^{-3} S cm^{-2}) and the subsequent fracture and pulverization of Si particles due to the enormous volume change severely restrict the rate performance [43,51]. In conclusion, silicon anodes' unique alloying method and greater Li storage potential, as well as their inhibition of lithium-ion accumulation at highly charged states, can improve fast-charging and diminish concentration and potential gradient effects that might cause capacity degradation during cycling.

5.1. Use of Silicon Carbon Composite for High-Energy and Fast-Charging LIBs

Since pure graphite anodes have practically attained their optimum performance, there has been much research over the past few decades on the incorporation of silicon in graphite composite electrodes. Increasing the capacity of anode is advantageous, and the impact is enhanced when cathode capacities are increased much beyond what is currently considered to be state-of-the-art. Specifically, the best strategy for preparing next-generation and fast-charging LIB anodes appears to be the incorporation of reasonable amounts of high-capacity anode materials like silicon, which has a theoretical capacity of 4200 mA h g^{-1}. Notably, using the material with the highest capacity known (Figure 6a) and with an average delithiation potential of ca. 0.4 V vs. Li/Li^+ in graphite-based composites for preparing next-generation and fast-charging LIB anodes [52]. For example, Jung et al. [53] developed encapsulated 50-nm-sized silicon nanoparticles (NPs) with nanoporous N-doped graphitic carbon along with dopamine polymer through polymerization and the addition of Fe^{3+} catalyst, followed by carbonization under controlled conditions (Figure 6b). The electrochemical performance of the as-synthesized silicon NPs with a graphitic carbon shell, as a LIB anode, indicated excellent high-rate capability and long-cycle stability. After 800 cycles at 2 A g^{-1}, the provided capacity was 1056 mA h g^{-1} (Figure 6c), and this excellent performance was attributable to the composite creation with graphene, which prevented significant volume changes during the charge/discharge process. In order to prevent capacity fading and restricted cycle life caused by unstable SEI formation, severe particle pulverization, and loss of electrical contact during charge/discharge, Jin et al. [54] also employed graphene addition with silicon. Ball-milling and subsequent Ag-assisted chemical etching were utilized to create porous silicon in a cost-effective and scalable manner. Upon chemical treatment and the adjustment of the reaction solutions, the morphology of porous silicon changed into a nanowire array (Figure 6d). To provide carbon coating to the porous silicon powder, the authors added graphene oxide solution to a mother solution in the ratio of 1:1 wt% under ultrasonic agitation for 1 h. Electrochemical analysis showed that the porous silicon structures with graphene incorporation could deliver a stable capacity of 1287 mAh g^{-1} over 100 cycles at a 2 A g^{-1} rate. Similarly, Yang et al. [55] prepared an anode through carbon coated mesoporous SiO_2 onto carbon nanotubes and subsequently converting into a meso-Si layer. The freestanding and highly porous sponge anode were connected through a sandwich-like carbon-Si-CNT structure. Li^+ diffusion was aided by the hierarchical sponge structure in the meso-Si layer, while electron transport was made easy by the CNT networks. The carbon coating on meso-Si also reduced the volume growth, which allowed for a high rate capability and a high specific capacity. Examples include the CNT/meso-Si/C composite anode, which demonstrated a discharge capacity

of 1700 mAh g^{-1} at a current density of 4 A g^{-1}, far greater than previous Si-based anodes (Figure 6e).

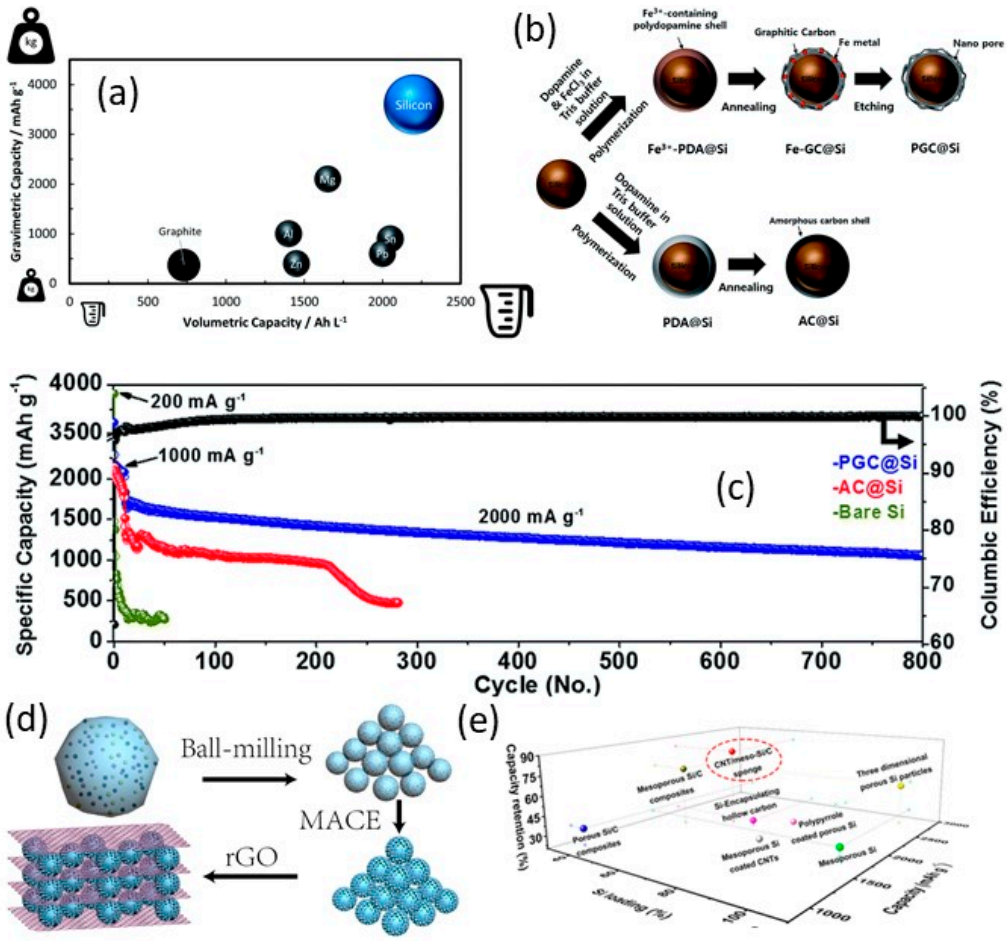

Figure 6. (**a**) Comparison of the gravimetric and volumetric capacity of some alloying elements along with graphite (Reprinted with permission from Ref. [26]. Copyright, 2020 Royal Society of Chemistry), (**b**) a schematic illustration of the preparation of nanoporous-graphitic-carbon-coated silicon NPs and amorphous-carbon-coated silicon NPs, (**c**) cycle stability of both samples, and bare Si electrodes (for comparison) at current densities of 0.2 (1 cycle), 1 (10 cycle), and 2 A g^{-1} for the rest of the cycles (Reprinted with permission from Ref. [53]. Copyright, 2018 Royal Society of Chemistry), (**d**) a schematic diagram of the simultaneous perforation and purification processes (Reprinted with permission from Ref. [52]. Copyright, 2015 American Chemical Society, Washington, DC, USA), and (**e**) comparison of the LIB performance between CNT/meso-Si/C sponge anode and other previously reported Si-based electrodes (Reprinted with permission from Ref. [55]. Copyright, 2017 American Chemical Society).

5.2. Nanosized Silicon Anode

A nano-scaled silicon anode has a low diffusion energy barrier, so lithium-ion has fast ion kinetics [56]. But, volume expansion during cycling and limitation of electrical conductivity is main challenges to commercial use of Silicon anode lithium-ion batteries. 3D Silicon nanowire (Si NWs) was introduced, because of many advantages. (1) lower diameter than bulk silicon, which means that volume expansion is suppressed during repeated charging and discharging process. (2) Each silicon nanowire directly contacts the current collector and shows high specific capacity. (3) Suitable for use with high rate performance due to 1D diffusion path. For example, Chan et al. synthesized Si NWs using the vapour–liquid–solid (VLS) process on stainless steel substrates using Au catalyst [57]. The electrochemical performance of Si NWs showed high cyclability and improved Li-

ion kinetics. After 20 cycles, the Si NWs anode has a capacity of over 3500 mAh g^{-1} under 0.84 A g^{-1}. The Si NWs also demonstrated high capacities (~2100 mAh g^{-1}) at 4.2 A g^{-1}. Despite Si NWs have been a lot of improvement compared to pure silicon, graphene, metal, metal oxide, polymer, and silicon oxide is needed to improve mechanical and electrical property of silicon anode. For example, Ren et al. introduced reduced Si NWs-Au-Reduced Graphene Oxide (Au-rGO). Using solvothermal method and CVD process Si NWs-Au-rGO composite was synthesized. SEM images showed that Si NWs are densely and randomly located on the rGO surface. The flexible Au-rGO with Si NWs maintains the structural integrity and provides a conductive network of the anode. As a result, Si NW-rGO composite electrodes retain a high specific capacity of 2300 mAh g^{-1} over 100 cycles [58]. And Lotfabad et al. improved Si NWs electrochemical properties via TiO_2 coating using atomic layer deposition (ALD). TiO_2 effectively suppresses particle pulverization and volume expansion. The capacity retention after 100 cycles for the TiO_2 coated Si NWs 60% at 0.42 A g^{-1} and 34% retention rate at higher current density (21 A g^{-1}). TiO_2 coating allows fast Li ion insertion/ extraction during continuous cycling.

In addition, Si nanotubes (NTs) as anodes in LIBs have been shown to increase battery performance, as reported by Cui's team as shown in Figure 7a [57]. Etching treatment was used after the Si NTs were produced through the reductive breakdown of a Si precursor in an alumina template. For this unique Si NT anode, battery testing revealed a high reversible charge capacity of 3247 mAh g^{-1} and a high Coulombic efficiency (CE) of 89%. Even at a high current density of 15 A g^{-1}, the synthesized Si CNT anode retained its capacity more effectively than other materials.

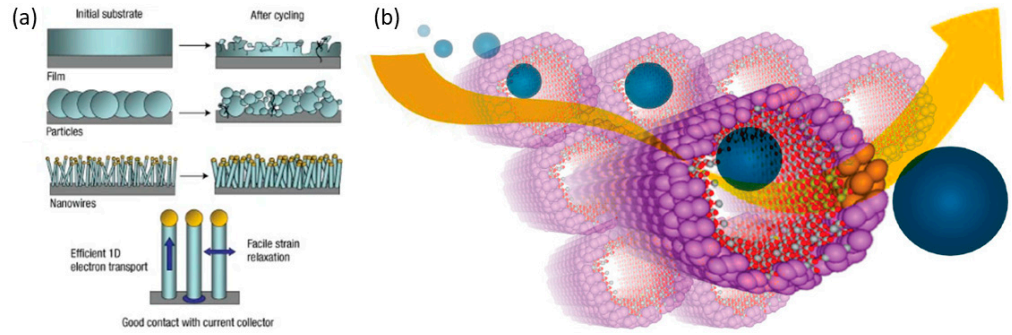

Figure 7. (**a**) Schematic of morphological changes that occur in Si during electrochemical cycling. (Reprinted with permission from Ref. [57]. Copyright, 2007 Nature Publishing). (**b**) Schematic diagram of Li-ion pathway in Si nanotubes. (Reprinted (adapted) with permission from Ref. [59]. Copyright, 2009 American Chemical Society).

5.3. Porous Silicon Anode

The structural stability of Si may be increased in a number of ways, including by the reduction in particle size and the introduction of empty spaces inside reSi particles. Introduced voids are able to support volume expansions of Si particles, resulting to improved structural integrity. It is common practice to classify methods for preparing porous Si into a top-down and a bottom-up category. To begin, micron-sized Si particles are used as a precursor in the top-down approach, and then electroless or electrochemical etching is used to produce empty spaces inside the particles. Additionally, the porous templates are used as a starting point for the bottom-up approach's templating procedure, which is then followed by Si deposition and the template-etching operations [24]. For instance, Zhou's team described a low-cost, top-down strategy to synthesis porous Si particles from metallurgical Si microparticles by ball milling and then treating them with an affordable stain-etching procedure (Figure 8A–E) [60]. The porous Si anode demonstrated a high reversible capacity of 2900 mAh g^{-1} at the current density of 400 mA g^{-1} and a sustained capacity of 1100 mAh g^{-1} after 600 cycle tests at 2000 mA g^{-1}. The amorphous silicon inverse opals were created by depositing Si on the porous templates using a chemical vapor deposition (CVD) technique (Figure 8F–H) [61]. It was found that the inverted opal

structure amorphous Si anode has good cycling properties. However, because of Si's poor conductivity, amorphous Si inverse opals don't work very well at high speeds.

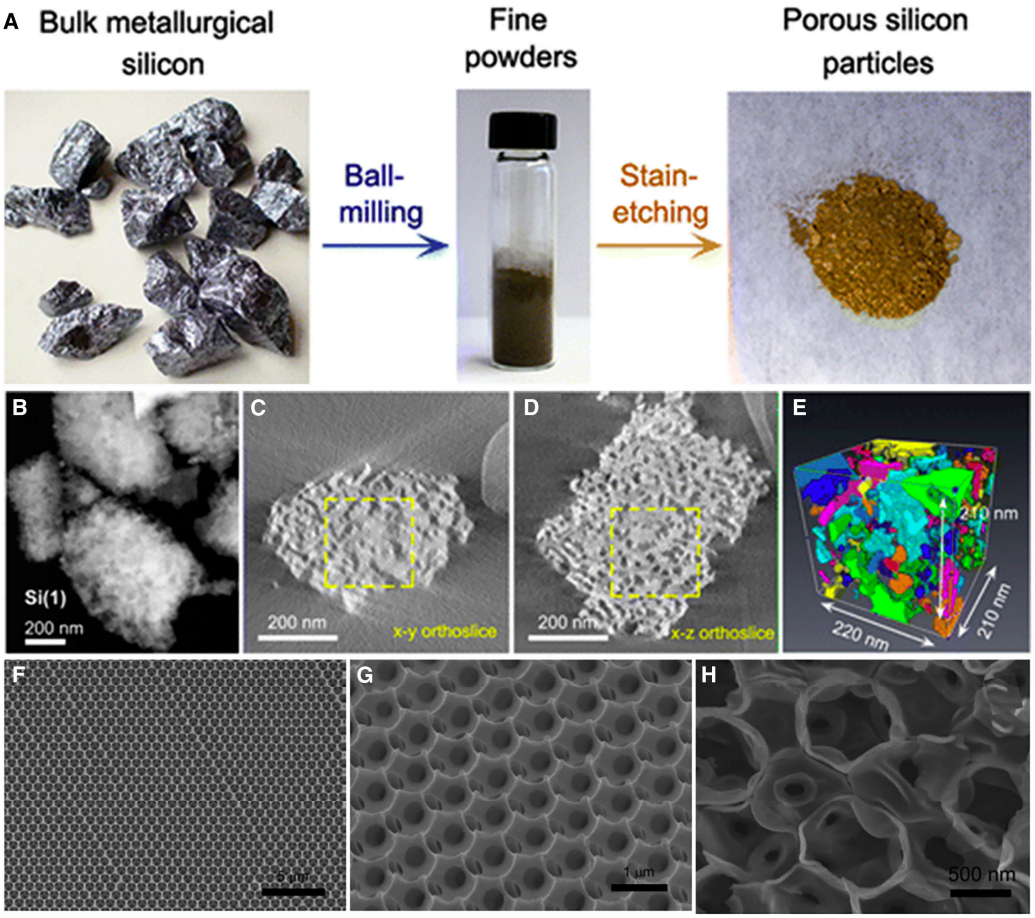

Figure 8. Structural characterization of porous Si anodes as (**A**) preparation process (**B**–**E**) Porous Si is reconstructed from HAADF-STEM tomography shown. (**F**–**H**) SEM images of porous Si templated from 890-nm pre-sintered silica microspheres before (**F**,**G**) and after (**H**) the CV test. (Reprinted with permission from Ref. [61]. Copyright, 2007 Elsevier).

5.4. Silicon-Derivative Materials

5.4.1. SiO_x

Silicon oxide (SiO_x, $0 < x \leq 2$) has recently been studied as a viable alternative for elemental Si due to its simple production, moderate theoretical volume expansion (118% for SiO compared to Si, ≥300%), and cheap cost [62]. The combination of Si-rich SiO_x ($x \leq 1$) with Gr has been a trend that has led to its commercialization in LIBs (typically SiO_x < 10 wt%) [63]. The SiO_x family consists of anode materials composed of silicon monoxide (SiO), silicon dioxide (SiO_2), non-stoichiometric SiO_x, and silicon oxycarbide (Si–O–C). The O concentration influences the specific capacity, cycle life, and voltage hysteresis (voltage hysteresis is the voltage differential between the charge and discharge profiles) [64]. For example, increased O contents result in longer cycle life and high-voltage hysteresis due to the release of strain and stress during the Li-ion insertion/extraction processes [65], while diminishing the initial Coulombic efficiency (ICE) and rate capability. This is mostly due to the irreversible consumption of Li^+ ions (e.g., forming Li_2O and Li_4SiO_4) [66].

5.4.2. SiN_x

Silicon nitride (SiN_x) is another family of Si derivatives that undergoes a two-stage reaction electrochemically, i.e., a conversion reaction leading to the formation of electro-

chemically stable and Li-ion conductive Li-Si-N compounds (e.g., Li_2SiN_2 [67]), followed by an alloying reaction, resulting in Si nanoparticles (SiNPs) [67–69]. When the nitrogen concentration of SiN_x is increased, the reversible capacity decreases with time, but the material becomes more stable during cycling and can handle higher cycling rates (both according to stoichiometry) [69]. The cycling performance of SiN_x electrodes [70] is profoundly influenced by the spatial distribution of Li silicon nitride products (Li_xSiN_y) following lithiation processes. Even if the results achieved in terms of cycle stability and rate capability were encouraging, Li-ion batteries with SiN_x anodes are not yet at a point where they can be sold commercially. Using powder-based electrodes and improving its poor first-cycle Coulombic efficiency (through additives, for example) are necessary steps toward incorporating SiN_x into functional cells [66].

6. Perspectives

Although LIBs have been improved to have an increased life cycle and to be more suitable for challenging environments, LIBs still lack fast-charging characteristics and safety. It has been shown that the introduction of carbon nanomaterials with silicon in the anode electrode not only maximizes the high capacity and durability by increasing the conductivity and flexibility and reducing the weight but also provides better safety [71]. As a result, LIB technology could be widely used for public and military applications. In fact, it is now apparent that carbon nanomaterial-containing silicon composites are promising materials for state-of-the-art next-generation LIBs for EVs, ESS, and military use, providing substantially enhanced energy densities, long durability, and safety, along with fast-charging properties.

However, there are some critical challenges related to fast-charging anode materials that should be overcome. For example, fast charging is generally impeded by the slow mass and charge transfer (refer to the Li^+) in electrode materials through the electrolyte. Important variables in attaining rapid charging include ensuring rapid Li^+ diffusion in the anode and decreasing the kinetic barrier between the anode and electrolyte contact. And the rate at which Li^+ and electrons are transferred within the solid electrode is affected by the ionic and electronic conductivity of the electrode materials. Therefore, improving conductivity is a fundamental strategy to improve the fast-charging capabilities, since it increases the Li^+ and electron mobility and ion diffusivity in the bulk of the materials and interface.

We reviewed the influence of diverse silicon anodes on rapid charging performance by incorporating silicon composite, silicon nanowire, porous silicon, and silicon-derivative materials (SiO_x, SiN_x). Nanosizing silicon anode reduces volume expansion while charging and increases reaction specific surface. Nanosizing silicon anodes offer stronger structural stability and Li^+ ion diffusivity than pure silicon, making them suitable for fast-charging LIBs. On Si-Carbon composite anode, Zhang's group coated metal oxide and achieved the high surface mechanical property [72]. Plasma treatments or chemical etching can boost the silicon anode's surface area and lithium-ion diffusion kinetics by creating a porous structure. By carefully tailoring the silicon anode and its surrounding components, next-generation fast-charging batteries may be able to attain high power and energy density. All Li and silicon alloy reactions occur at the interface between the electrolyte and anode. Therefore, improving interface modification is a fundamental strategy to improve fast-charging capabilities.

However, there are some critical challenges related to fast-charging anode materials that must be overcome. Slow mass transfer and charge transfer of Li^+ in electrode materials through the electrolyte, high Li^+ activation barriers for reaction, and low ion and electronic conductivity are the main problems to address. All Li and silicon alloy reactions occur at the interface between the electrolyte and anode. Therefore, improving interface modification is a fundamental strategy to improve fast-charging capabilities. These challenges can be solved by Size control, Oxygen control, Pre-lithiation, Li trapping control, Nano-porous Si design, Surface modification of nanosized silicon, Nanosized silicon/graphite composite

electrode design, advanced binding, and Advanced electrolyte additives. In this paper, we have discussed most of the solutions for silicon future batteries.

To achieve rapid charging, it is also necessary to enhance the SEI layer by making it mechanically stable and allowing for superior ion conductivity. A better fit between electrolyte composition and material structure can also be used to enhance the fundamental features of the SEI layer. Li^+ migration to the anode and desolvation and passage via the SEI should both be fast during rapid charging. Thus, materials with huge porosity, high surface area, and flexibility are highly recommended since these characteristics are favorable for stable SEI formation and volume change mitigation. Finally, for achieving fast charging, high density, long-lasting, and safe LIBs, intensive research should be conducted on every component of the batteries since the anode, cathode, and electrolyte materials eventually control the entire battery chemistry. By addressing the challenges associated with fast-charging anode materials, significant progress can be made toward the development of efficient and sustainable energy storage systems.

Author Contributions: J.-Y.H. proposed concept, supervision and wrote an original manuscript. J.L. and G.O. wrote a manuscript and organize reference. H.-Y.J. review the manuscript and funding acquisition. All authors have read and agreed to the published version of the manuscript.

Funding: This research receives no external funding.

Acknowledgments: This work was supported by the Agency for Defense Development by the Korean Government (UD2200061D) and National Research Foundation of Korea (NRF) grant funded by the Korean government (MSIT) (Grant Nos. NRF-2022R1C1C1011058).

Conflicts of Interest: The authors declare no conflict of interest.

References

1. Larcher, D.; Tarascon, J.-M. Towards Greener and More Sustainable Batteries for Electrical Energy Storage. *Nat. Chem.* **2015**, *7*, 19–29. [CrossRef] [PubMed]
2. Duan, J.; Tang, X.; Dai, H.; Yang, Y.; Wu, W.; Wei, X.; Huang, Y. Building Safe Lithium-Ion Batteries for Electric Vehicles: A Review. *Electrochem. Energy Rev.* **2020**, *3*, 1–42. [CrossRef]
3. Dunn, J.B.; Gaines, L.; Kelly, J.C.; James, C.; Gallagher, K.G. The Significance of Li-Ion Batteries in Electric Vehicle Life-Cycle Energy and Emissions and Recycling's Role in Its Reduction. *Energy Environ. Sci.* **2014**, *8*, 158–168. [CrossRef]
4. Li, M.; Lu, J.; Chen, Z.; Amine, K. 30 Years of Lithium-Ion Batteries. *Adv. Mater.* **2018**, *30*, 1800561. [CrossRef]
5. Global EV Outlook 2021—Analysis. Available online: https://www.iea.org/reports/global-ev-outlook-2021 (accessed on 9 February 2023).
6. Dunn, B.; Kamath, H.; Tarascon, J.-M. Electrical Energy Storage for the Grid: A Battery of Choices. *Science* **2011**, *334*, 928–935. [CrossRef]
7. Pan, H.; Hu, Y.-S.; Chen, L. Room-Temperature Stationary Sodium-Ion Batteries for Large-Scale Electric Energy Storage. *Energy Environ. Sci.* **2013**, *6*, 2338–2360. [CrossRef]
8. Li, S.; Wang, K.; Zhang, G.; Li, S.; Xu, Y.; Zhang, X.; Zhang, X.; Zheng, S.; Sun, X.; Ma, Y. Fast Charging Anode Materials for Lithium-Ion Batteries: Current Status and Perspectives. *Adv. Funct. Mater.* **2022**, *32*, 2200796. [CrossRef]
9. Ahmed, M.S.; Lee, S.; Agostini, M.; Jeong, M.-G.; Jung, H.-G.; Ming, J.; Sun, Y.-K.; Kim, J.; Hwang, J.-Y. Multiscale Understanding of Covalently Fixed Sulfur–Polyacrylonitrile Composite as Advanced Cathode for Metal–Sulfur Batteries. *Adv. Sci.* **2021**, *8*, 2101123. [CrossRef]
10. Irle, R. Global EV Sales for 2022. Available online: https://www.ev-volumes.com (accessed on 9 February 2023).
11. Li, W.; Dahn, J.R.; Wainwright, D.S. Rechargeable Lithium Batteries with Aqueous Electrolytes. *Science* **1994**, *264*, 1115–1118. [CrossRef]
12. Tran, M.; Banister, D.; Bishop, J.D.K.; McCulloch, M.D. Realizing the Electric-Vehicle Revolution. *Nat. Clim. Chang.* **2012**, *2*, 328–333. [CrossRef]
13. Thakur, A.K.; Ahmed, M.S.; Oh, G.; Kang, H.; Jeong, Y.; Prabakaran, R.; Vikram, M.P.; Sharshir, S.W.; Kim, J.; Hwang, J.-Y. Advancement in Graphene-Based Nanocomposites as High Capacity Anode Materials for Sodium-Ion Batteries. *J. Mater. Chem. A* **2021**, *9*, 2628–2661. [CrossRef]
14. Thakur, A.K.; Ahmed, M.S.; Park, J.; Prabakaran, R.; Sidney, S.; Sathyamurthy, R.; Kim, S.C.; Periasamy, S.; Kim, J.; Hwang, J.-Y. A Review on Carbon Nanomaterials for K-Ion Battery Anode: Progress and Perspectives. *Int. J. Energy Res.* **2022**, *46*, 4033–4070. [CrossRef]
15. Liu, W.; Placke, T.; Chau, K.T. Overview of Batteries and Battery Management for Electric Vehicles. *Energy Rep.* **2022**, *8*, 4058–4084. [CrossRef]

16. Gohier, A.; Laïk, B.; Kim, K.-H.; Maurice, J.-L.; Pereira-Ramos, J.-P.; Cojocaru, C.S.; Van, P.T. High-Rate Capability Silicon Decorated Vertically Aligned Carbon Nanotubes for Li-Ion Batteries. *Adv. Mater.* **2012**, *24*, 2592–2597. [CrossRef] [PubMed]
17. Xia, S.; Mu, L.; Xu, Z.; Wang, J.; Wei, C.; Liu, L.; Pianetta, P.; Zhao, K.; Yu, X.; Lin, F.; et al. Chemomechanical Interplay of Layered Cathode Materials Undergoing Fast Charging in Lithium Batteries. *Nano Energy* **2018**, *53*, 753–762. [CrossRef]
18. Yan, P.; Zheng, J.; Gu, M.; Xiao, J.; Zhang, J.-G.; Wang, C.-M. Intragranular Cracking as a Critical Barrier for High-Voltage Usage of Layer-Structured Cathode for Lithium-Ion Batteries. *Nat. Commun.* **2017**, *8*, 14101. [CrossRef]
19. Vetter, J.; Novák, P.; Wagner, M.R.; Veit, C.; Möller, K.-C.; Besenhard, J.O.; Winter, M.; Wohlfahrt-Mehrens, M.; Vogler, C.; Hammouche, A. Ageing Mechanisms in Lithium-Ion Batteries. *J. Power Sources* **2005**, *147*, 269–281. [CrossRef]
20. Campion, C.L.; Li, W.; Lucht, B.L. Thermal Decomposition of $LiPF_6$-Based Electrolytes for Lithium-Ion Batteries. *J. Electrochem. Soc.* **2005**, *152*, A2327. [CrossRef]
21. Waldmann, T.; Hogg, B.-I.; Wohlfahrt-Mehrens, M. Li Plating as Unwanted Side Reaction in Commercial Li-Ion Cells—A Review. *J. Power Sources* **2018**, *384*, 107–124. [CrossRef]
22. Hall, D.S.; Eldesoky, A.; Logan, E.R.; Tonita, E.M.; Ma, X.; Dahn, J.R. Exploring Classes of Co-Solvents for Fast-Charging Lithium-Ion Cells. *J. Electrochem. Soc.* **2018**, *165*, A2365. [CrossRef]
23. Nazari, A.; Farhad, S. Heat Generation in Lithium-Ion Batteries with Different Nominal Capacities and Chemistries. *Appl. Therm. Eng.* **2017**, *125*, 1501–1517. [CrossRef]
24. Ge, M.; Fang, X.; Rong, J.; Zhou, C. Review of Porous Silicon Preparation and Its Application for Lithium-Ion Battery Anodes. *Nanotechnology* **2013**, *24*, 422001. [CrossRef]
25. Salah, M.; Murphy, P.; Hall, C.; Francis, C.; Kerr, R.; Fabretto, M. Pure Silicon Thin-Film Anodes for Lithium-Ion Batteries: A Review. *J. Power Sources* **2019**, *414*, 48–67. [CrossRef]
26. Asenbauer, J.; Eisenmann, T.; Kuenzel, M.; Kazzazi, A.; Chen, Z.; Bresser, D. The Success Story of Graphite as a Lithium-Ion Anode Material—Fundamentals, Remaining Challenges, and Recent Developments Including Silicon (Oxide) Composites. *Sustain. Energy Fuels* **2020**, *4*, 5387–5416. [CrossRef]
27. Zhang, R.; Du, Y.; Li, D.; Shen, D.; Yang, J.; Guo, Z.; Liu, H.K.; Elzatahry, A.A.; Zhao, D. Highly Reversible and Large Lithium Storage in Mesoporous Si/C Nanocomposite Anodes with Silicon Nanoparticles Embedded in a Carbon Framework. *Adv. Mater.* **2014**, *26*, 6749–6755. [CrossRef]
28. Su, X.; Wu, Q.; Li, J.; Xiao, X.; Lott, A.; Lu, W.; Sheldon, B.W.; Wu, J. Silicon-Based Nanomaterials for Lithium-Ion Batteries: A Review. *Adv. Energy Mater.* **2014**, *4*, 1300882. [CrossRef]
29. Kulova, T.L.; Skundin, A.M.; Pleskov, Y.V.; Terukov, E.I.; Kon'kov, O.I. Lithium Insertion into Amorphous Silicon Thin-Film Electrodes. *J. Electroanal. Chem.* **2007**, *600*, 217–225. [CrossRef]
30. Ko, M.; Chae, S.; Cho, J. Challenges in Accommodating Volume Change of Si Anodes for Li-Ion Batteries. *ChemElectroChem* **2015**, *2*, 1645–1651. [CrossRef]
31. Wu, J.; Cao, Y.; Zhao, H.; Mao, J.; Guo, Z. The Critical Role of Carbon in Marrying Silicon and Graphite Anodes for High-Energy Lithium-Ion Batteries. *Carbon Energy* **2019**, *1*, 57–76. [CrossRef]
32. Duan, H.; Xu, H.; Wu, Q.; Zhu, L.; Zhang, Y.; Yin, B.; He, H. Silicon/Graphite/Amorphous Carbon as Anode Materials for Lithium Secondary Batteries. *Molecules* **2023**, *28*, 464. [CrossRef]
33. Liu, G.; Yang, Y.; Lu, X.; Qi, F.; Liang, Y.; Trukhanov, A.; Wu, Y.; Sun, Z.; Lu, X. Fully Active Bimetallic Phosphide $Zn_{0.5}Ge_{0.5}P$: A Novel High-Performance Anode for Na-Ion Batteries Coupled with Diglyme-Based Electrolyte. *ACS Appl. Mater. Interfaces* **2022**, *14*, 31803–31813. [CrossRef] [PubMed]
34. Su, Y.-S.; Hsiao, K.-C.; Sireesha, P.; Huang, J.-Y. Lithium Silicates in Anode Materials for Li-Ion and Li Metal Batteries. *Batteries* **2022**, *8*, 2. [CrossRef]
35. Mei, Y.; He, Y.; Zhu, H.; Ma, Z.; Pu, Y.; Chen, Z.; Li, P.; He, L.; Wang, W.; Tang, H. Recent Advances in the Structural Design of Silicon/Carbon Anodes for Lithium Ion Batteries: A Review. *Coatings* **2023**, *13*, 436. [CrossRef]
36. Saager, S.; Decker, L.; Kopte, T.; Scheffel, B.; Zimmermann, B. High-Performance Anodes Made of Metallic Lithium Layers and Lithiated Silicon Layers Prepared by Vacuum Technologies. *Batteries* **2023**, *9*, 75. [CrossRef]
37. Heß, M.; Novák, P. Shrinking Annuli Mechanism and Stage-Dependent Rate Capability of Thin-Layer Graphite Electrodes for Lithium-Ion Batteries. *Electrochim. Acta* **2013**, *106*, 149–158. [CrossRef]
38. Feng, X.; Bai, Y.; Liu, M.; Li, Y.; Yang, H.; Wang, X.; Wu, C. Untangling the Respective Effects of Heteroatom-Doped Carbon Materials in Batteries, Supercapacitors and the ORR to Design High Performance Materials. *Energy Environ. Sci.* **2021**, *14*, 2036–2089. [CrossRef]
39. Wang, A.; Kadam, S.; Li, H.; Shi, S.; Qi, Y. Review on Modeling of the Anode Solid Electrolyte Interphase (SEI) for Lithium-Ion Batteries. *npj Comput. Mater.* **2018**, *4*, 15. [CrossRef]
40. Heiskanen, S.K.; Kim, J.; Lucht, B.L. Generation and Evolution of the Solid Electrolyte Interphase of Lithium-Ion Batteries. *Joule* **2019**, *3*, 2322–2333. [CrossRef]
41. Zheng, L.; Guo, F.; Kang, T.; Fan, Y.; Gu, W.; Mao, Y.; Liu, Y.; Huang, R.; Li, Z.; Shen, Y.; et al. Stable Lithium-Carbon Composite Enabled by Dual-Salt Additives. *Nano-Micro Lett.* **2021**, *13*, 111. [CrossRef]
42. Han, B.; Liao, C.; Dogan, F.; Trask, S.E.; Lapidus, S.H.; Vaughey, J.T.; Key, B. Using Mixed Salt Electrolytes to Stabilize Silicon Anodes for Lithium-Ion Batteries via in Situ Formation of Li–M–Si Ternaries (M = Mg, Zn, Al, Ca). *ACS Appl. Mater. Interfaces* **2019**, *11*, 29780–29790. [CrossRef]

43. Yazami, R.; Touzain, P. A Reversible Graphite-Lithium Negative Electrode for Electrochemical Generators. *J. Power Sources* **1983**, *9*, 365–371. [CrossRef]
44. Chae, S.; Ko, M.; Kim, K.; Ahn, K.; Cho, J. Confronting Issues of the Practical Implementation of Si Anode in High-Energy Lithium-Ion Batteries. *Joule* **2017**, *1*, 47–60. [CrossRef]
45. Sandhya, C.P.; John, B.; Gouri, C. Lithium Titanate as Anode Material for Lithium-Ion Cells: A Review. *Ionics* **2014**, *20*, 601–620. [CrossRef]
46. Selinis, P.; Farmakis, F. Review—A Review on the Anode and Cathode Materials for Lithium-Ion Batteries with Improved Subzero Temperature Performance. *J. Electrochem. Soc.* **2022**, *169*, 010526. [CrossRef]
47. Lee, J.-I.; Ko, Y.; Shin, M.; Song, H.-K.; Choi, N.-S.; Gyu Kim, M.; Park, S. High-Performance Silicon-Based Multicomponent Battery Anodes Produced via Synergistic Coupling of Multifunctional Coating Layers. *Energy Environ. Sci.* **2015**, *8*, 2075–2084. [CrossRef]
48. Xia, Q.; Xu, A.; Du, L.; Yan, Y.; Wu, S. High-Rate, Long-Term Performance of LTO-Pillared Silicon/Carbon Composites for Lithium-Ion Batteries Anode under High Temperature. *J. Alloys Compd.* **2019**, *800*, 50–57. [CrossRef]
49. Maibach, J.; Lindgren, F.; Eriksson, H.; Edström, K.; Hahlin, M. Electric Potential Gradient at the Buried Interface between Lithium-Ion Battery Electrodes and the SEI Observed Using Photoelectron Spectroscopy. *J. Phys. Chem. Lett.* **2016**, *7*, 1775–1780. [CrossRef]
50. Casimir, A.; Zhang, H.; Ogoke, O.; Amine, J.C.; Lu, J.; Wu, G. Silicon-Based Anodes for Lithium-Ion Batteries: Effectiveness of Materials Synthesis and Electrode Preparation. *Nano Energy* **2016**, *27*, 359–376. [CrossRef]
51. Huang, G.; Han, J.; Lu, Z.; Wei, D.; Kashani, H.; Watanabe, K.; Chen, M. Ultrastable Silicon Anode by Three-Dimensional Nanoarchitecture Design. *ACS Nano* **2020**, *14*, 4374–4382. [CrossRef]
52. Li, X.; Zhang, M.; Yuan, S.; Lu, C. Research Progress of Silicon/Carbon Anode Materials for Lithium-Ion Batteries: Structure Design and Synthesis Method. *ChemElectroChem* **2020**, *7*, 4289–4302. [CrossRef]
53. Jung, C.-H.; Choi, J.; Kim, W.-S.; Hong, S.-H. A Nanopore-Embedded Graphitic Carbon Shell on Silicon Anode for High Performance Lithium Ion Batteries. *J. Mater. Chem. A* **2018**, *6*, 8013–8020. [CrossRef]
54. Jin, Y.; Zhang, S.; Zhu, B.; Tan, Y.; Hu, X.; Zong, L.; Zhu, J. Simultaneous Purification and Perforation of Low-Grade Si Sources for Lithium-Ion Battery Anode. *Nano Lett.* **2015**, *15*, 7742–7747. [CrossRef] [PubMed]
55. Yang, Y.; Yang, X.; Chen, S.; Zou, M.; Li, Z.; Cao, A.; Yuan, Q. Rational Design of Hierarchical Carbon/Mesoporous Silicon Composite Sponges as High-Performance Flexible Energy Storage Electrodes. *ACS Appl. Mater. Interfaces* **2017**, *9*, 22819–22825. [CrossRef]
56. Zhao, X.; Lehto, V.-P. Challenges and Prospects of Nanosized Silicon Anodes in Lithium-Ion Batteries. *Nanotechnology* **2020**, *32*, 042002. [CrossRef] [PubMed]
57. Chan, C.K.; Peng, H.; Liu, G.; McIlwrath, K.; Zhang, X.F.; Huggins, R.A.; Cui, Y. High-Performance Lithium Battery Anodes Using Silicon Nanowires. *Nat. Nanotechnol.* **2008**, *3*, 31–35. [CrossRef] [PubMed]
58. Ren, J.-G.; Wang, C.; Wu, Q.-H.; Liu, X.; Yang, Y.; He, L.; Zhang, W. A silicon nanowire-reduced graphene oxide composite as a high-performance lithium ion battery anode material. *Nanoscale* **2014**, *6*, 3353–3360. [CrossRef]
59. Park, M.-H.; Kim, M.G.; Joo, J.; Kim, K.; Kim, J.; Ahn, S.; Cui, Y.; Cho, J. Silicon Nanotube Battery Anodes. *Nano Lett.* **2009**, *9*, 3844–3847. [CrossRef]
60. Ge, M.; Lu, Y.; Ercius, P.; Rong, J.; Fang, X.; Mecklenburg, M.; Zhou, C. Large-Scale Fabrication, 3D Tomography, and Lithium-Ion Battery Application of Porous Silicon. *Nano Lett.* **2014**, *14*, 261–268. [CrossRef]
61. Esmanski, A.; Ozin, G.A. Silicon Inverse-Opal-Based Macroporous Materials as Negative Electrodes for Lithium Ion Batteries. *Adv. Funct. Mater.* **2009**, *19*, 1999–2010. [CrossRef]
62. Pan, K.; Zou, F.; Canova, M.; Zhu, Y.; Kim, J.-H. Systematic Electrochemical Characterizations of Si and SiO Anodes for High-Capacity Li-Ion Batteries. *J. Power Sources* **2019**, *413*, 20–28. [CrossRef]
63. Choi, J.W.; Aurbach, D. Promise and Reality of Post-Lithium-Ion Batteries with High Energy Densities. *Nat. Rev. Mater.* **2016**, *1*, 16013. [CrossRef]
64. Liu, Z.; Yu, Q.; Zhao, Y.; He, R.; Xu, M.; Feng, S.; Li, S.; Zhou, L.; Mai, L. Silicon Oxides: A Promising Family of Anode Materials for Lithium-Ion Batteries. *Chem. Soc. Rev.* **2019**, *48*, 285–309. [CrossRef] [PubMed]
65. Kim, M.K.; Jang, B.Y.; Lee, J.S.; Kim, J.S.; Nahm, S. Microstructures and Electrochemical Performances of Nano-Sized SiO_x ($1.18 \leq x \leq 1.83$) as an Anode Material for a Lithium(Li)-Ion Battery. *J. Power Sources* **2013**, *244*, 115–121. [CrossRef]
66. Eshetu, G.G.; Zhang, H.; Judez, X.; Adenusi, H.; Armand, M.; Passerini, S.; Figgemeier, E. Production of High-Energy Li-Ion Batteries Comprising Silicon-Containing Anodes and Insertion-Type Cathodes. *Nat. Commun.* **2021**, *12*, 5459. [CrossRef] [PubMed]
67. Ulvestad, A.; Mæhlen, J.P.; Kirkengen, M. Silicon Nitride as Anode Material for Li-Ion Batteries: Understanding the SiN_x Conversion Reaction. *J. Power Sources* **2018**, *399*, 414–421. [CrossRef]
68. Ulvestad, A.; Andersen, H.F.; Jensen, I.J.T.; Mongstad, T.T.; Mæhlen, J.P.; Prytz, Ø.; Kirkengen, M. Substoichiometric Silicon Nitride—An Anode Material for Li-Ion Batteries Promising High Stability and High Capacity. *Sci. Rep.* **2018**, *8*, 8634. [CrossRef] [PubMed]
69. de Guzman, R.C.; Yang, J.; Cheng, M.M.-C.; Salley, S.O.; Ng, K.Y.S. High Capacity Silicon Nitride-Based Composite Anodes for Lithium Ion Batteries. *J. Mater. Chem. A* **2014**, *2*, 14577–14584. [CrossRef]

70. Chae, S.; Park, S.; Ahn, K.; Nam, G.; Lee, T.; Sung, J.; Kim, N.; Cho, J. Gas Phase Synthesis of Amorphous Silicon Nitride Nanoparticles for High-Energy LIBs. *Energy Environ. Sci.* **2020**, *13*, 1212–1221. [CrossRef]
71. Liu, H.; Chen, T.; Xu, Z.; Liu, Z.; Yang, J.; Chen, J. High-Safety and Long-Life Silicon-Based Lithium-Ion Batteries via a Multifunctional Binder. *ACS Appl. Mater. Interfaces* **2020**, *12*, 54842–54850. [CrossRef]
72. Zhang, Q.; Xi, B.; Chen, W.; Feng, J.; Qian, Y.; Xiong, S. Synthesis of Carbon Nanotubes-Supported Porous Silicon Microparticles in Low-Temperature Molten Salt for High-Performance Li-Ion Battery Anodes. *Nano Res.* **2022**, *15*, 6184–6191. [CrossRef]